https://doi.org/10.5194/egusphere-2024-3207
Preprint. Discussion started: 8 November 2024

Evaluation of high-intensity rainfall observations from personal weather stations in the Netherlands

Nathalie Rombeek[1], Markus Hrachowitz[1], Arjan Droste[1], and Remko Uijlenhoet[1]
[1]Department of Water Management, Delft University of Technology, the Netherlands
Correspondence: Nathalie Rombeek (n.rombeek@tudelft.nl)

Abstract. Accurate rainfall observations with a high spatial and temporal resolution are key for hydrological applications, in particular for reliable flood forecasts. However, rain gauge networks operated by regional or national environmental agencies are often sparse and weather radars tend to underestimate rainfall. As a complementary source of information, rain gauges from personal weather stations (PWSs), which have a network density 100 times higher than dedicated rain gauge networks in the Netherlands, can be used. However, PWSs are prone to additional sources of error compared to dedicated gauges, because they are generally not installed and maintained according to international guidelines. Here, we quantitatively compare rainfall estimates obtained from PWSs against rainfall recorded by automatic weather stations (AWSs) from the Royal Netherlands Meteorological Institute (KNMI), over the 2018-2023 period, including a sample of 1760 individual rainfall events in the Netherlands. This sample consists of the 10 highest rainfall accumulations per season and accumulation interval (1, 3, 6 and 24 h) over a 6-year period. It was found that the average of a cluster of PWSs severely underestimate rainfall (around 36% and 19% for 1 h and 24 h intervals, respectively). Adjusting the data with the mean field bias correction factor of 1.24, as proposed by the PWSQC algorithm, reduces this underestimation to 21% for 1 h intervals or almost reduces it to 0 for intervals of 3 h and longer. Largest correlation (0.83 and 0.83) and lowest coefficient of variation (0.15 and 0.18) were found during winter and autumn, respectively. We show that most PWSs are able to capture high rainfall intensities up to around 30 mm h^{-1}, indicating that these can be utilized for applications that require rainfall data with with a spatial resolution on the order of kilometers, such as for flood forecasting in small, fast responding catchments. However, PWSs severely underestimate (on average more than 50%) rainfall events with return periods exceeding 10 or 50 years (above approximately 30 mm h^{-1}), which occurred in spring and summer. These underestimations are associated with large areal reduction factors, which can result in a reduction up to 17% for 1 h events with a return period of 50 years. Additionally, this undercatch is likely due to the disproportional underestimation of tipping bucket rain gauges with increasing intensities. We recommend additional research on dynamic calibration of the tipping volumes to further improve this. Outliers during winter were likely caused by solid precipitation and can potentially be removed using a temperature module from the PWS.

1 Introduction

Accurate rainfall observations are essential for hydrological applications, such as flood forecasting. However, rainfall is highly variable in time and space, making it challenging to capture its dynamics accurately. Consequently, the stochastic nature of

https://doi.org/10.5194/egusphere-2024-3207
Preprint. Discussion started: 8 November 2024

rainfall is one of the main sources of uncertainty in hydrological modeling (Niemczynowicz, 1999; Moulin et al., 2009; Arnaud et al., 2011; Lobligeois et al., 2014; Beven, 2016; McMillan et al., 2018). Especially small, fast-responding catchments require accurate rainfall observations with a high spatial and temporal resolution for reliable predictions (e.g. in the order of kilometers and minutes for catchments areas of around 560 ha) (Berne et al., 2004; Ochoa-Rodriguez et al., 2015; Cristiano et al., 2017; Thorndahl et al., 2017). To reduce the uncertainty of catchment-scale rainfall estimates, accurate instruments with a high spatio-temporal resolution are required.

Rain gauges and weather radars are widely used instruments to provide rainfall information for hydrological forecasting. Each instrument has its own advantages and limitations. Rain gauges can record rainfall relatively accurately at the point-scale. These rain gauges can be automatic or manual, observing at short regular intervals (e.g. recorded every 12 sec, archived at 10 min time steps in the Netherlands) or daily, respectively. A limitation is that these measurements are strictly only representative for the orifice area of the individual recording gauge and the network density of dedicated rain gauges is not sufficient to capture small-scale rainfall dynamics (Villarini et al., 2008; Hrachowitz and Weiler, 2011; Van Leth et al., 2021). In addition, rainfall observations from manual gauges, which are emptied in a measuring cylinder and read once a day, are not available in (near) real time. Weather radars, on the other hand, provide high spatial and temporal resolution data (i.e. typically 1 km^2 and 5 min), that is available in near real-time. However, radar rainfall estimates are prone to substantial uncertainty and bias due to several sources of error. These are related to both the instrument itself (e.g. calibration) and to the conversion from measured reflectivities aloft into rainfall rates at the ground (Uijlenhoet and Berne, 2008; Krajewski et al., 2010; Villarini and Krajewski, 2010).

Alternatively, crowdsourced rain measurements, in the form of low-cost weather observation devices, may potentially provide accurate local rainfall observations. These devices are referred to as personal weather stations (PWSs) and can contain a rain gauge module, which records rainfall at a high temporal resolution (5 min). The popularity of these low-cost rainfall sensors has been increasing in the last decade, up to around 1 PWS per 9, 11, 13 and 15 km^2 in May 2024, in the Netherlands, Denmark, Switzerland and Germany, respectively. Figure 1 shows several tens of thousands PWSs with varying densities across Europe, with more than 60% having 5 or more neighbouring stations within 10 km. In the Netherlands, these sensors currently have a network density which is about 100 times higher than that of the AWSs, with even higher densities in urban areas, where AWS densities are typically low (Overeem et al., 2024b; Brousse et al., 2024). The data from these observations is automatically uploaded to different online platforms such as the Weather Observations Website (WOW; https://wow.metoffice.gov.uk/), the Weather Underground website (https://www.wunderground.com/wundermap) and Netatmo (https://weathermap.netatmo.com/). The PWS data is open access and in case of Netatmo it can be extracted in near real-time using an application programming interface (API) every 5 min. However, since they are installed, operated and maintained largely by non-specialist citizens, the data quality of these PWSs is expected to be lower than that of professionally operated gauges of national meteorological or hydrological services.

Rain gauges, both PWS and AWS, are prone to several sources of error. These errors can be grouped into three categories: (1) instrumental, such as calibration errors or the intrinsic tipping bucket error, meaning that a given volume of water needs to be collected before it tips (Habib et al., 2001) or; (2) data processing, such as rounding or connectivity issues during

https://doi.org/10.5194/egusphere-2024-3207
Preprint. Discussion started: 8 November 2024

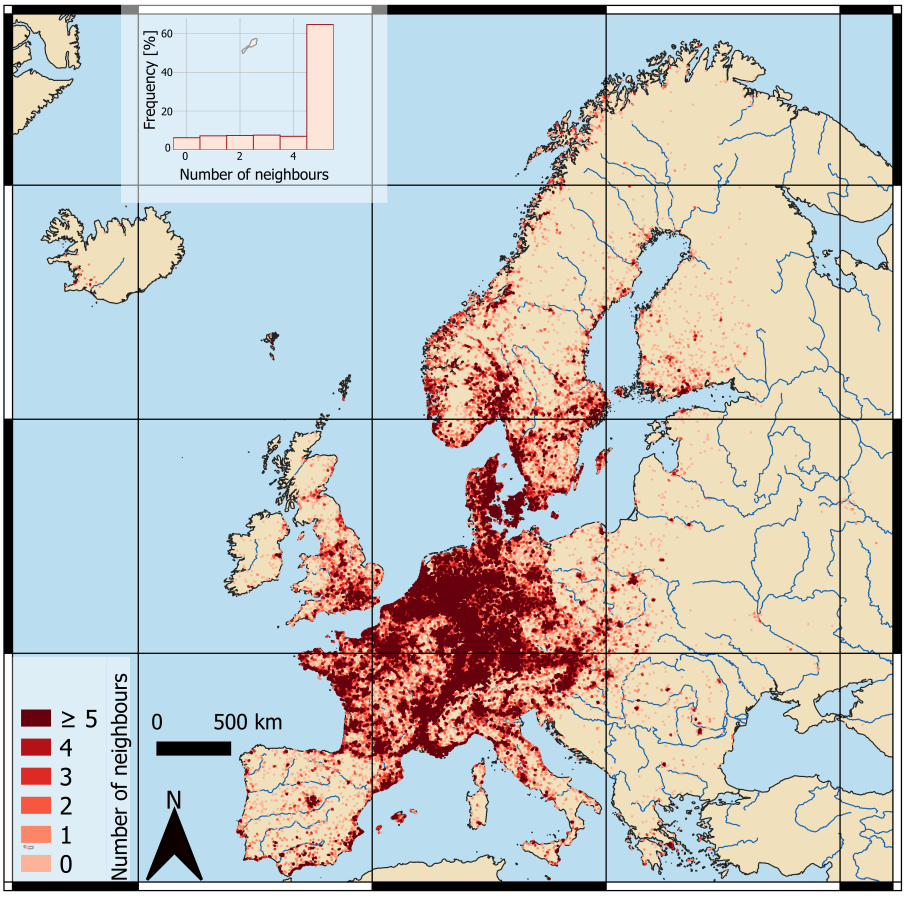

Figure 1. Indication of the Netatmo density of PWSs with rain gauges within Europe, showing number of PWS neighbours within a radius of 10 km. Data extracted from netatmo API on April 2024.

data transfer and (3) setup and maintenance. In addition, uncertainties arise due to spatial sampling errors resulting from estimating areal rainfall using point measurements (Villarini et al., 2008). Rain gauges of PWSs typically uses a tipping bucket mechanism to record the rainfall volumes. The quality of rainfall intensity estimates from these mechanisms has been shown to be intensity-dependent. Tipping buckets are known to overestimate rainfall at low intensities and underestimate for high intensities (Marsalek, 1981; Shedekar et al., 2009; Colli et al., 2014), which are part of the first category of errors. In addition, these errors can be amplified if the PWSs are not installed correctly and maintained adequately.

With respect to the first two sources of error, De Vos et al. (2017) used an experimental setup to investigate part of the instrument and data processing-related errors from PWSs. They showed that, under ideal circumstances (i.e. installed and maintained according to World Meteorological Organization standards), three rain gauges, from the Netatmo brand, recorded rainfall with high accuracy. Collocating the PWSs very close to one of KNMI's automatic weather stations (AWSs), spatial sampling errors were also limited. Despite the potential of accurate rainfall measurements from PWSs, their observations

https://doi.org/10.5194/egusphere-2024-3207
Preprint. Discussion started: 8 November 2024

are often not optimal, as the stations are not necessarily installed according to guidelines from the World Meteorological Organization. To account for those, errors related to the third category are introduced. For that reason, De Vos et al. (2019) developed a quality control (QC) algorithm, to filter outliers from the PWS network without using data from an official rain gauge network or weather radar. Similarly, Bárdossy et al. (2021) developed a QC algorithm, using a reference observation network to filter outliers and to correct the bias.

While implementing these QC algorithms has been shown to yield an overall improvement in the quality of the PWS data (De Vos et al., 2019; Bárdossy et al., 2021; Overeem et al., 2024a; Nielsen et al., 2024; El Hachem et al., 2024, in press), a systematic long-term analysis for different seasons, accumulation intervals and intensity classes is missing so far. In particular, a focus on high rainfall intensities is important, as the undercatch of rain gauges is likely disproportional with increasing intensities. Here, we aim to quantitatively compare rain data from PWSs with AWSs, extending on the results of De Vos et al. (2017, 2019). While weather radar data has a larger spatial resolution compared to AWSs, it is not used in this research as a reference because it is prone to several sources of error and therefore significantly underestimates rainfall. Note that in previous research from Overeem et al. (2024a) rainfall estimates from PWSs were actually used to correct a rainfall radar product.

The objective of this study is to systematically quantify and describe the uncertainties arising from PWS rainfall estimates. By analyzing the 10 largest rainfall accumulations, with return periods up to 50 years, during the period between 2018 and 2023, for 11 AWSs, 4 seasons and 4 time intervals, we can draw statistically meaningful conclusions on this. To the best of the authors' knowledge, such long-term study using PWS data that focuses on the most intense rainfall events, has not been performed before. Quantifying the limitations the PWS rainfall observations and eventually correcting it, maximizes the potential of PWSs for (hydrological) forecasts.

2 Study area and data

This study was carried out over the period 2018-2023 in the Netherlands, which has a land surface area of approximately 35,000 km^2 (Fig. 3a). This period was chosen due to PWS data availability, which increased over the years. The Netherlands has a maritime climate (Cfb according to the Köppen classification), where winters are mild, with an average temperature of 3.8 °C and relatively cool summers (17.2 °C) (KNMI, 2024). The average yearly rainfall between 1990-2020 is 851 mm yr^{-1} over the area (KNMI, 2024). In addition, regional variability in rainfall extremes is observed, with higher values in the western part of the country (Overeem et al., 2009; Beersma et al., 2019). The Dutch climate has a quite uniform distribution of precipitation over the meteorological seasons, except during spring, which is the driest season and contains the driest month (i.e. April, average 41 mm) (see Fig 2). August is on average the wettest month (average 87.4 mm) (KNMI, 2024). However, rainfall characteristics differ over the seasons. Rainfall during the summer months and beginning of autumn is characterized by shorter duration and higher precipitation intensities, as a consequence of convection during these months. In contrast, during the winter months lower intensities and more frequent and longer precipitation events occur (De Vries and Selten, 2023).

https://doi.org/10.5194/egusphere-2024-3207
Preprint. Discussion started: 8 November 2024

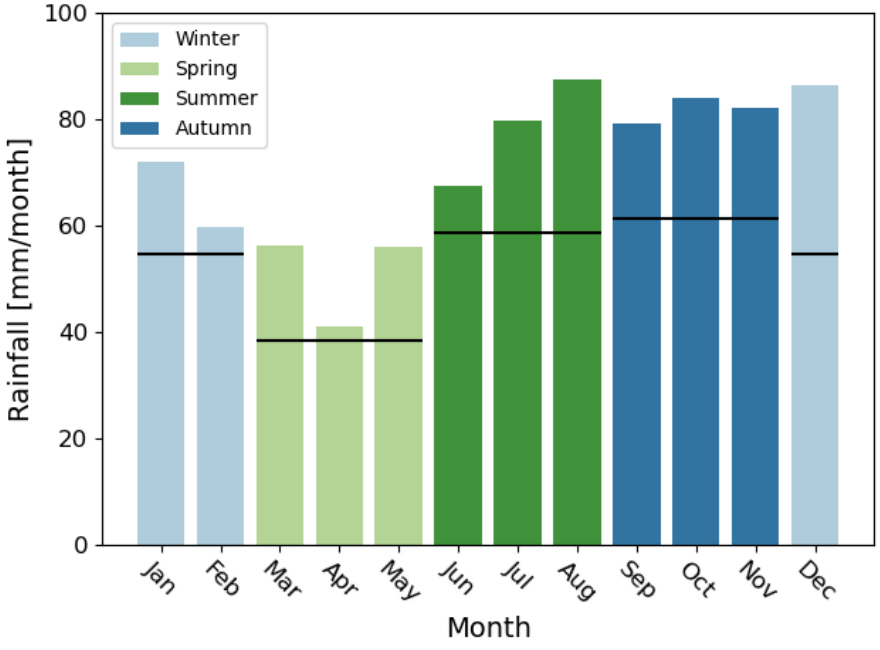

Figure 2. Average rainfall per month and season in the Netherlands over the period 1991-2020, based on data from 13 stations spread over the country, obtained from KNMI (2024). Coloured bars indicate the average rainfall per month (left y-axis, mm month^{-1}), horizontal black lines the average rainfall over each season.

2.1 Personal weather stations

For the analysis here rain gauges from the Netatmo brand of PWSs were used. These PWSs have a large coverage over the Netherlands which slightly increased since 2018 (around one PWS per 9 km^2 in 2024; Fig. 3a). This rain gauge type uses a tipping bucket mechanism with a nominal volume of 0.101 mm according to the manufacturer (Netatmo, 2024a). These gauges can also be calibrated manually by the owner, resulting in deviating tipping bucket volumes (approximately 13.5% is manually calibrated according to De Vos et al. (2019)). The default rain gauge processing software records the number of tips over 5 min intervals, which is communicated wirelessly to an indoor module. Next, the data is transferred, using wifi, to the Netatmo platform. The diameter of the collecting funnel is 13 cm (leading to an orifice area of 133 cm^2). According to the manufacturer, the accuracy is 1 mm h^{-1} for a measurement range of 0.2 to 150 mm h^{-1} and the PWS operates best for temperatures between 0 and 50°C (Netatmo, 2024a). However, it is unclear what this accuracy exactly entails, therefore pointing out the need for this study.

https://doi.org/10.5194/egusphere-2024-3207
Preprint. Discussion started: 8 November 2024

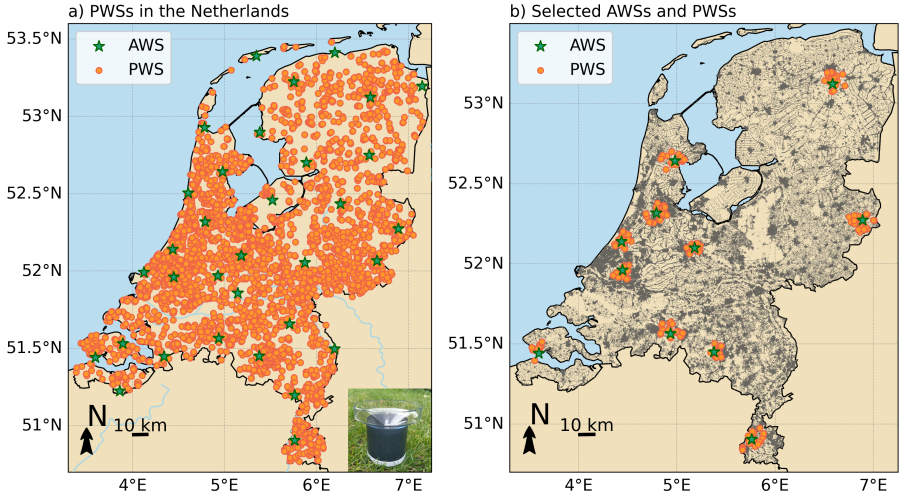

Figure 3. Map of the Netherlands showing a) the locations of the 33 AWSs employed by KNMI and the locations of available PWSs in 2024 obtained using the Netatmo API (approximately 4000 PWSs) (Netatmo (2024b) last access: 08/05/2024). The photo in the right corner shows an example of the PWS used in this research. Note that working PWSs in 2024 are not part of the dataset in this study. b) The selected AWSs and PWSs from 2018 to 2023 in this study. Built-up areas, indicated in grey, were obtained from European Environment Agency (2020).

2.2 Reference dataset

The PWSs were evaluated against data from automatic weather stations (AWSs) from the Royal Netherlands Meteorological Institute (KNMI). The KNMI operates a network of 33 AWSs across the Netherlands, which are relatively homogeneously distributed, with approximately one AWS per 1000 km^2 (Fig. 3a). These AWSs estimate cumulative rainfall every 12 s by measuring the displacement of a float placed in a reservoir. The collecting funnel has a diameter of 16 cm (corresponding to an orifice area of 201 cm^2) and the device is heated for temperatures below 4°C. In addition, these stations are placed in open locations using an English setup or Ott windscreen to reduce errors from wind induced undercatch (Brandsma et al., 2020). The data is archived at a lower resolution, i.e. every 1 min, 10 min and hourly. Here, AWS data with a resolution of 10 min and 1 h is used. The 10 min dataset contains unvalidated rainfall data, while the hourly data has been validated (Brandsma et al., 2020).

3 Methods

3.1 Station selection

Rainfall data at 5-min intervals from multiple PWSs were extracted using the Netatmo API (Netatmo, 2024b). Netatmo limits the API requests per hour. Note that the API only provides PWSs that are operational at time of access, which was in February 2024, meaning we do not have the exact recording stations, which varied over time. Two search radii were employed to find

https://doi.org/10.5194/egusphere-2024-3207
Preprint. Discussion started: 8 November 2024

all operational PWSs within that range. One radius of 10 km around an AWS was used for quantifying the quality of PWSs and a radius of 20 km for filtering the PWS data using a quality control algorithm. Van de Beek et al. (2012) and Van Leth et al. (2021) showed that the decorrelation distance for precipitation over the Netherlands is around 50 km for 1 h accumulation intervals. Comparing PWSs within 10 km from an AWSs can therefore be assumed to limit spatial sampling errors with respect to a larger search radius.

First, all PWSs within 20 km around each AWS were identified. Secondly, AWSs that had at least 5 PWSs within 10 km since 2018-01-01 were kept in the dataset. Next, the 10 closest available PWSs located within 10 km from the AWS were selected (Fig. 4, purple crosses) for the comparison with the AWS nearby. Note that the selection of PWSs varies per selected rainfall event, due to temporary station outages and changing data and station availability over time. This procedure resulted in 11 AWSs with a cluster of 5 to 10 PWSs around it (Fig. 3b for selected AWSs and used PWSs). All PWSs within 20 km were used for filtering the data (Fig. 4, orange dots and purple crosses) using the quality control algorithm developed by De Vos et al. (2019) and described below (Sect. 3.3).

3.2 Event selection

A similar event selection procedure was used as described by Imhoff et al. (2020), which defines an event as a certain time period, rather than by the beginning and end of rainfall. Rainfall observations from the AWSs were employed to make a selection of events between 2018 and 2023. Only the largest rainfall accumulations were selected, as these are the most important ones for pluvial flood forecasting. Analysis shows that, on average, the 10 highest 1-h rainfall accumulations for the selected AWSs account or 12.5% of the annual rainfall. The 10-min dataset of the AWSs was used to select these events, the hourly dataset was employed to perform a consistency check on this selection. For selected events with rainfall differences of more than 10% with the validated hourly dataset, the values of the validated hourly dataset were used instead. These deviations occurred in less than 0.4% of the total selected events. Note that the selected events can contain time steps without any rain observed.

For every selected AWS based on the methodology in Section 3.1, the 10 largest rainfall events per meteorological season (winter, spring, summer and autumn) and per accumulation interval (1, 3, 6 and 24 hours) were selected to draw statistically meaningful conclusions. This results in a total of 11 stations x 4 seasons x 4 accumulation intervals x 10 events = 1760 individual events for the analysis. The events were selected in such way that for the same station and accumulation interval no overlapping time series were selected.

The statistics of the selected events are shown in Fig. 5. A clear seasonality is observed here, especially for 1 h intervals (Fig. 5a), with highest rates during summer (JJA) and lowest during winter (DJF), with a median of 14.65 and 6.17 mm h^{-1}, respectively. This is aligned with the Dutch climate, where highest rainfall intensities occur during summer and are typically characterized by convective rainfall (Beersma et al., 2019).

Based on the return periods provided by Beersma et al. (2019), over 75% of the selected observed rainfall accumulations in winter, spring and autumn have a return period of less than 0.5 year, while in summer this is around 25% (Fig. 5a). Most extreme events occur during the summer months, with multiple events having a return period of over 5 years, and one event exceeding a return period of 100 years. Rainfall rates during the autumn months (SON) are slightly higher compared to spring (MAM),

https://doi.org/10.5194/egusphere-2024-3207
Preprint. Discussion started: 8 November 2024

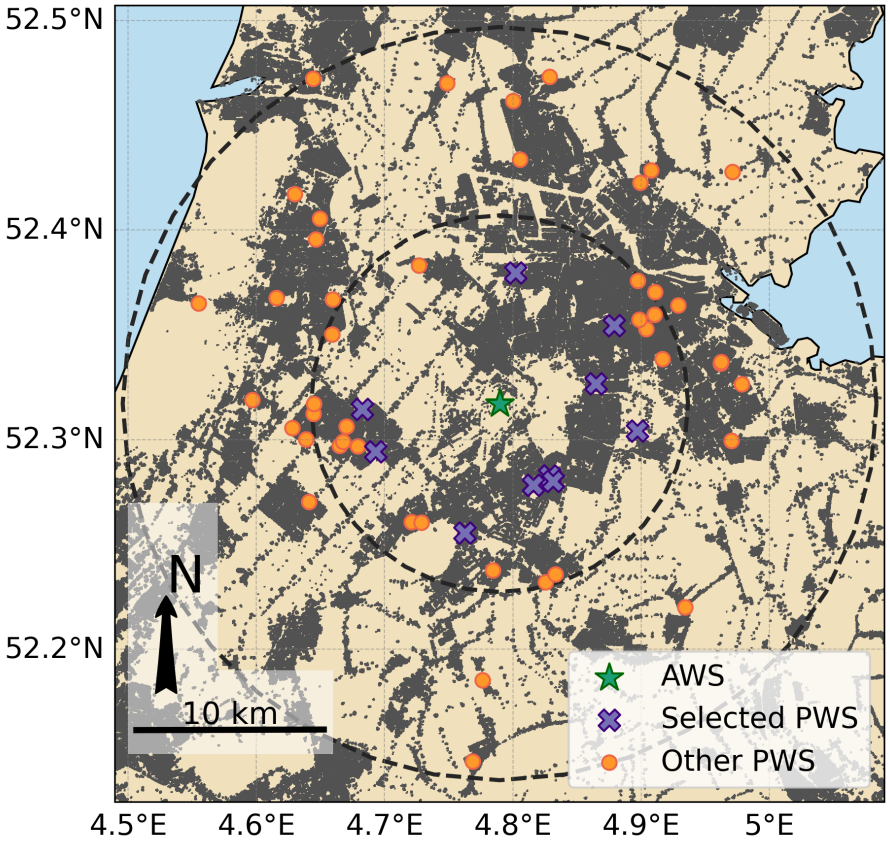

Figure 4. Example of the selection procedure for the AWS at Schiphol. The green star indicates the AWS operated by KNMI, the purple crosses indicate the 10 closest PWSs within a distance of 10 km around the AWS. The orange dots are the other PWSs within 20 km from the AWS, which are utilized for quality control. Built-up areas, indicated in grey, were obtained from European Environment Agency (2020).

for example with a median of 9.40 and 8.33 mm h^{-1}, respectively (Fig. 5a). However, spring appears to have two extreme outliers, with return periods that exceed 10 years. Note that these return periods are calculated based on annual statistics, which is dominated by rainfall events during March until October. Because winter has the lowest intensities, return periods in winter based on annual statistics are low.

3.3 Quality control algorithm

Part of the quality control algorithm PWSQC from De Vos et al. (2019) was applied to filter the PWS dataset, using the same parameters. First, a list of PWS neighbours was constructed. Secondly, high influx (HI) and faulty zeroes (FZ) filters were computed for every timestep (i.e. 5 min). High influx data can be caused by sprinklers, adding liquids into the gauge, or tilting of the gauge. Faulty zeroes can result from failure of the tipping bucket mechanism. At least five neighbouring PWSs must be present to attribute the HI and FZ flags, otherwise the value will be eliminated from the dataset. Time steps that were flagged

https://doi.org/10.5194/egusphere-2024-3207
Preprint. Discussion started: 8 November 2024

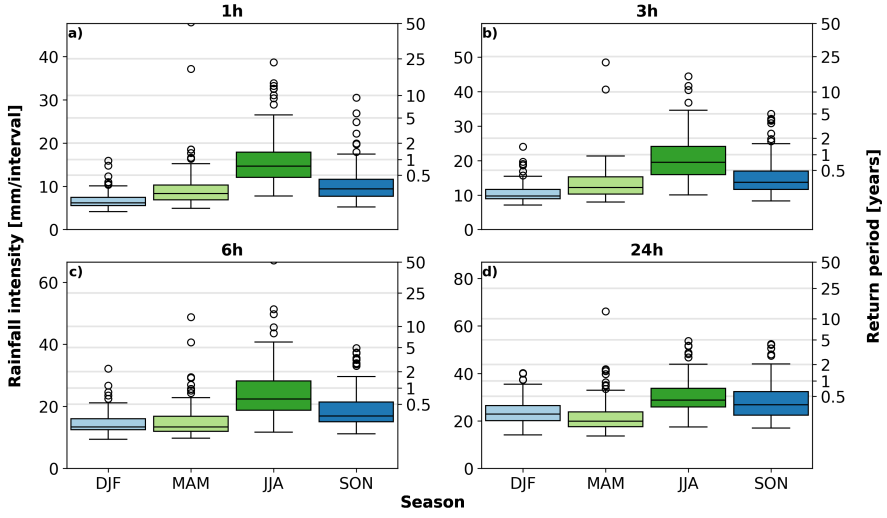

Figure 5. Mean rainfall intensity [mm/interval] for the different selected events per season (11 AWSs x 10 rainfall events) for the four accumulation intervals (1, 3, 6 and 24 h). Left y-axis shows the rainfall over the specific interval, right y-axis indicate the different corresponding return periods for the intensities reported by Beersma et al. (2019). The lower and upper whiskers indicate the minimum and maximum intensities and the boxes the inter-percentile range (25^{th}–75^{th}). During summer outliers were present, with return periods larger than 50 years.

according to the HI or FZ flags were removed. As a last step of the PWSQC algorithm, a default bias correction factor of 1.24 was applied to the dataset. This factor is based on correcting the bias over an entire area, rather than addressing individual biases in PWSs. For this reason, we refer to it in this research as mean field bias correction (MFBC).

3.4 Network stability

Over time the availability of PWSs changes due to factors such as connection failure. To analyze the availability of PWSs, a dataset comprising operational PWSs at 2018-01-01 within 10 km from an AWS were employed. This dataset contained 178 PWSs. Time series from the PWSs were extracted for each selected event according to the method described in Section 3.2. In total, 95.8% of the PWSs were available over all selected events during the 6 consecutive years. From these available PWSs, 3.5% of the total time steps did not contain any data. In addition, 0.7% of the PWSs did not have 5 neighbours within 10 km. Applying the quality control algorithm leads to discarding more data. For the remaining PWSs with enough neighbours, 8.9% of the total data is either discarded (i.e. flagged as FZ or HI) or missing.

A minimum percentage of time steps should be valid before aggregating the data. The criteria set has a large impact on the availability (Table 1). By requiring a data availability of 100% before aggregation, 40.9% of the dataset is retained, while a lower required availability (92%) almost doubles (79.7%) the remaining stations of the original dataset. Lower criteria potentially result in underestimation of rainfall due to missing data. Based on these results, a data availability requirement of 83% was chosen to keep a large part of the original dataset (83.7%), which is also in line with Overeem et al. (2024a).

https://doi.org/10.5194/egusphere-2024-3207
Preprint. Discussion started: 8 November 2024

Table 1. Percentage of the PWSs available (28,480 different PWS time series) over all selected events after flagging data and setting a minimum availability criteria.

Availability criteria	Remaining PWSs
100%	40.9%
92%	79.9%
83%	83.7%
75%	85.8%

3.5 Validation

The data quality of the PWSs was evaluated by comparing the PWS data to those of the selected AWSs, using the relative bias, coefficient of variation (CV) of the residuals, the Pearson correlation coefficient (r), and the slope of linear regression relationship. Note that the evaluation metrics were calculated over the total rainfall within a time interval and over the average of the cluster of PWSs.

The bias was defined as follows:

$$\text{Bias} = \frac{\sum_{i=1}^{n} R_{\text{PWS},i}}{\sum_{i=1}^{n} R_{\text{AWS},i}} - 1, \tag{1}$$

with n the total number of events for each season and time interval, and R_{AWS} and R_{PWS} the rain recorded by the AWS and PWS respectively. The CV is used to describe the dispersion of rainfall, and is defined as follows:

$$\text{CV} = \frac{\sqrt{\frac{1}{n}\sum_{i=1}^{n}(R_{\text{res},i} - \overline{R}_{\text{res}})^2}}{\overline{R_{\text{AWS}}}}, \tag{2}$$

with

$$R_{\text{res}} = R_{\text{PWS}} - R_{\text{AWS}}. \tag{3}$$

The Pearson correlation coefficient describes the strength of the linear relation between the PWSs and the AWS and was calculated between all events within a season and aggregation interval (including zeroes):

$$r = \frac{\text{cov}(R_{\text{PWS}}, R_{\text{AWS}})}{\text{sd}(R_{\text{PWS}})\text{sd}(R_{\text{AWS}})}. \tag{4}$$

The linear regression line, fitted through the origin, is defined as follows:

$$\overline{R_{\text{PWS}}} = a * \overline{R_{\text{AWS}}}, \tag{5}$$

https://doi.org/10.5194/egusphere-2024-3207
Preprint. Discussion started: 8 November 2024

with a the slope calculated over all events:

$$a = \frac{\sum_{i=1}^{n} R_{\mathrm{AWS},i} R_{\mathrm{PWS},i}}{\sum_{i=1}^{n} (R_{\mathrm{AWS},i})^2}. \tag{6}$$

3.6 Areal reduction factor

While the AWS represents a point measurement, which has a limited spatial footprint, it is compared to average rainfall over a domain (i.e. a cluster of PWSs around an AWS). With increasing domain area, the variation of areal precipitation becomes smaller than that of point precipitation. To account for the reduction in the magnitude of rainfall extremes over an area as compared to a point, areal reduction factors (ARF) can be applied. The ARF estimates areal rainfall percentiles from point rainfall percentiles. Overeem et al. (2010) and more recently Beersma et al. (2019) parameterized the ARF based on weather radar for the Netherlands. This reduction factor is a function of duration, area and return period, with rarer events having a stronger areal reduction. Equations 1a, 2, 3b, 4 and 5 from Beersma et al. (2019) are used to estimate the ARF.

4 Results

After applying the HI and FZ filters and requiring a minimum data availability before aggregation, around 88% of the original dataset was kept.

4.1 Spatial sampling

The PWSs in this study were selected based on the closest distance from an AWS, without considering the uniformity of distribution around the AWS. Figure 6 shows that the average cluster distance towards an AWS is around 4.5 km and that the average intergauge PWSs distance of all pairs within a cluster is around 5 km. This indicates that overall, the selected stations are not clustered at one location and represent a larger area. Variation in the distance towards the AWSs in Fig. 6a can be explained due to the location of the selected AWSs. Higher PWS network densities and associated shorter distances to the closest PWSs can be found in urban regions. However, most of the AWSs are located in rural regions. In addition, variability in Fig. 6 also partially results from fluctuating data availability and number of available PWSs, which increases over the years. The average number of PWSs within a cluster is 8.75.

4.2 Bias

To highlight the severity of the bias in the PWSs, no MFBC factor was applied initially. The bias of the PWSs over multiple accumulation intervals was quantified by comparing it with AWSs nearby for the selected rainfall events (Table 2, each row indicating different accumulation intervals). Results indicate that, on average, significant biases are present in rainfall observations from the PWSs. The underestimation is largest for accumulation intervals of 1 h (around 36%). The magnitude of the bias reduces over longer intervals, towards an underestimation of around 19% for accumulation intervals of 24 h.

https://doi.org/10.5194/egusphere-2024-3207
Preprint. Discussion started: 8 November 2024

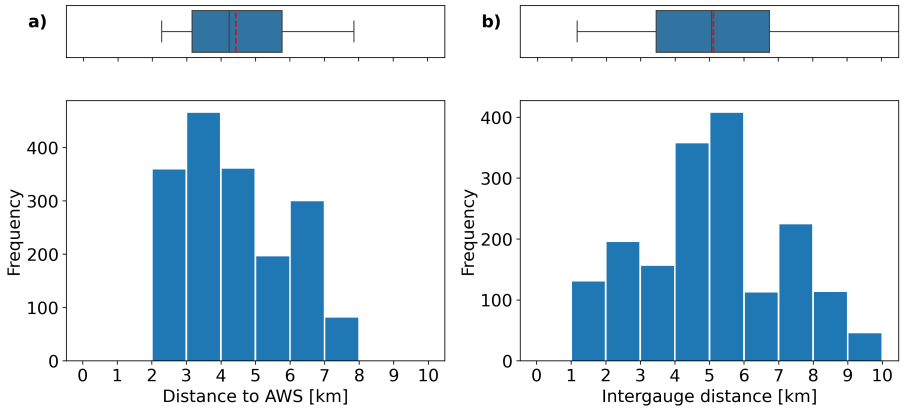

Figure 6. Histogram of a) distances between the PWS clusters and the AWSs per event and b) the inter-station distances between all selected PWS pairs within a cluster per event, both based on 1760 pairs. Vertical red dashed line indicates the mean distance, vertical black line the median, the left and right whiskers indicate the minimum and maximum distance and boxes the inter-percentile range (25^{th}–75^{th}).

These results indicate the need for a MFBC factor, with more significant adjustment required for shorter accumulation intervals. To compensate for this bias, the MFBC of 1.24, proposed by De Vos et al. (2019) as part of their quality control algorithm, was applied. After application of the MFBC, the underestimation for 1 h intervals reduces to an average of 21%, while for 24 h it converges towards zero. This is supporting evidence that the MFBC works effectively for longer accumulation intervals, however, a significant underestimation remains for 1-h intervals, requiring a higher MFBC factor to correct for the substantial underestimation.

A small part of the raw dataset obtained from Netatmo (5.38% of the selected events' total time steps) was not available. Part of the underestimation with respect to the AWSs can be attributed to these missing time steps in the PWS dataset. Missing observations in the PWS dataset result in lower rainfall estimates compared to a complete dataset. However, the extent of the underestimation cannot be determined, as these time steps are missing.

4.3 Seasonal dependence

For the selected events, a seasonal dependency is visible for the performance of the PWSs (Figs. 7 and 8). The seasonal effect is most pronounced for shorter accumulation intervals (1 h and 3 h), with the best performance of the PWSs in winter and autumn and worst in summer and spring (Fig. 8). Events in winter show the lowest variability of the PWS observations compared with the AWS observations (e.g. CV of 0.27 and 0.20 for accumulation intervals of 1 h and 3 h, respectively). While the CV is slightly larger for autumn (0.34 and 0.24), the correlation between the PWSs and AWS is higher during autumn compared to winter (Fig. 8b). Winter in the Netherlands is mainly characterized by larger, more persistent rainfall systems, which have a longer decorrelation distance (80 km for 1-h aggregations) (Van de Beek et al., 2012). In addition, the error bars for winter are smaller compared to the other seasons, showing that there is more consistency between the individual PWSs (see supporting information Fig.A1 for a complete overview of all seasons and accumulation intervals). For that reason, it is expected that

https://doi.org/10.5194/egusphere-2024-3207
Preprint. Discussion started: 8 November 2024

Table 2. Relative bias calculated before and after applying the MFBC of 1.24 from De Vos et al. (2019) over the 110 (i.e. 10 rainfall events x 11 AWSs) selected rainfall events per season and interval.

	Relative bias [-]			
Interval	**DJF**	**MAM**	**JJA**	**SON**
No MFBC				
1 h	−0.33	−0.39	−0.38	−0.34
3 h	−0.22	−0.26	−0.27	−0.21
6 h	−0.20	−0.23	−0.21	−0.20
24 h	−0.18	−0.21	−0.19	−0.18
MFBC = 1.24				
1 h	−0.17	−0.24	−0.23	−0.18
3 h	−0.03	−0.08	−0.09	−0.03
6 h	−0.01	−0.05	−0.02	−0.01
24 h	0.02	−0.02	0.01	0.02

the spatial sampling errors were minimized during winter, indicating that other factors, such as solid rain, caused the lower correlation.

Figure 8a shows that for all seasons, the CV reduces over longer accumulation intervals. For 1-h intervals the CV varies over the different seasons between 0.27 and 0.55, while for 24 h the CV shows lower variability, with values varying between 0.15 and 0.27. Similarly, the correlation coefficient increases from values ranging from 0.36 to 0.71 for 1-h intervals to a range from 0.70 to 0.83 for 24-h intervals. This indicates that, for longer accumulation intervals, rainfall observations from PWSs exhibit less variability and more agreement with those from AWSs. Data transferring and processing errors reduces for longer accumulation intervals, as the effect of incorrectly attributing rainfall to a certain time stamp decreases. Overall, the average of the cluster of PWSs largely follows the 1:1 line, with slopes of the fitted lines indicating slight underestimation or overestimation by varying between 0.95 and 1.02 for 24 h. Furthermore, high correlations, low CV-values and low biases are found for both winter and autumn, indicating that there is a good agreement with the AWSs (Fig. 8).

4.4 Outlier identification

Figure 7 shows that, for certain individual events, the PWSs report rainfall amounts which deviate strongly from those observed by the AWSs. We further investigated the cause of some of these outliers, which are indicated with orange circles.

It can be seen in Fig. 7c that one of the selected events showed (almost) zero precipitation measurements according to the cluster of PWSs, while the AWS nearby recorded precipitation. These outliers occurred during winter and were also observed for the 6 h accumulation interval. In the Netherlands, winter has on average around 34 days with a minimum temperature below 0°C (KNMI, 2024), which is outside the optimal temperature range of the PWSs. For the event with the outliers in Fig. 7c, the maximum temperature was below -1.4 °C. If these events were discarded by a temperature filter that filters stations when

https://doi.org/10.5194/egusphere-2024-3207
Preprint. Discussion started: 8 November 2024

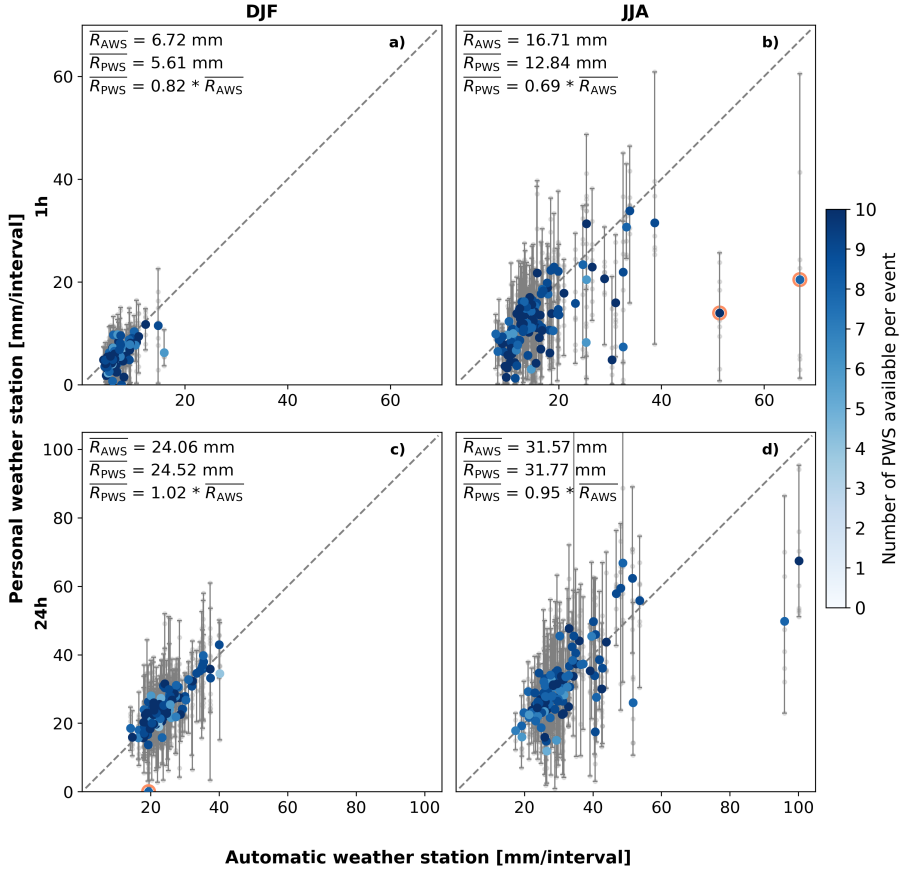

Figure 7. Scatter plots of filtered PWS rainfall accumulations against AWS records for the winter (a, c) and summer (b, d) seasons and accumulation intervals of 1 h (a, b) and 24 h (c, d). The large blue dots indicate the average of a cluster of PWS against one AWS, the vertical bars indicate the minimum and maximum of that cluster of PWSs. The blue gradient indicates the number of PWSs used to calculate the mean, minimum and maximum rainfall. The small grey dots indicate one individual PWS against an AWS. Orange circles indicate examples of outliers. The $\overline{R_{\mathrm{AWS}}}$ and $\overline{R_{\mathrm{PWS}}}$ represent the average rainfall over the selected events recorded by the AWS and PWS, respectively. $\overline{R_{\mathrm{PWS}}} = a * \overline{R_{\mathrm{AWS}}}$ represents the linear regression line, fitted through zero, with a indicating the slope.

temperatures are below a certain threshold for a certain duration, the values of r and CV for 6 h for winter would have improved to 0.81 and 0.17, respectively. For 24 h this would have been r = 0.86 and CV = 0.12. However, as these are only two points and the two intervals have some overlap in time at the same location, no statistically valid conclusion can be drawn from this.

The highest rainfall accumulations were observed during summer and spring, with an average intensity of more than 35 mm h^{-1}. An example of the low performance of PWSs for two high rainfall events in summer can be seen from Fig. 7b. These events influence the overall performance during these months. This suggests PWSs have difficulties recording higher rainfall intensities, which is known for tipping bucket mechanisms. In addition, PWSs only sends rainfall data to the netatmo platform twice per 10 min, which is considerable lower than the recording interval of AWSs (12 sec). More than one third

https://doi.org/10.5194/egusphere-2024-3207
Preprint. Discussion started: 8 November 2024

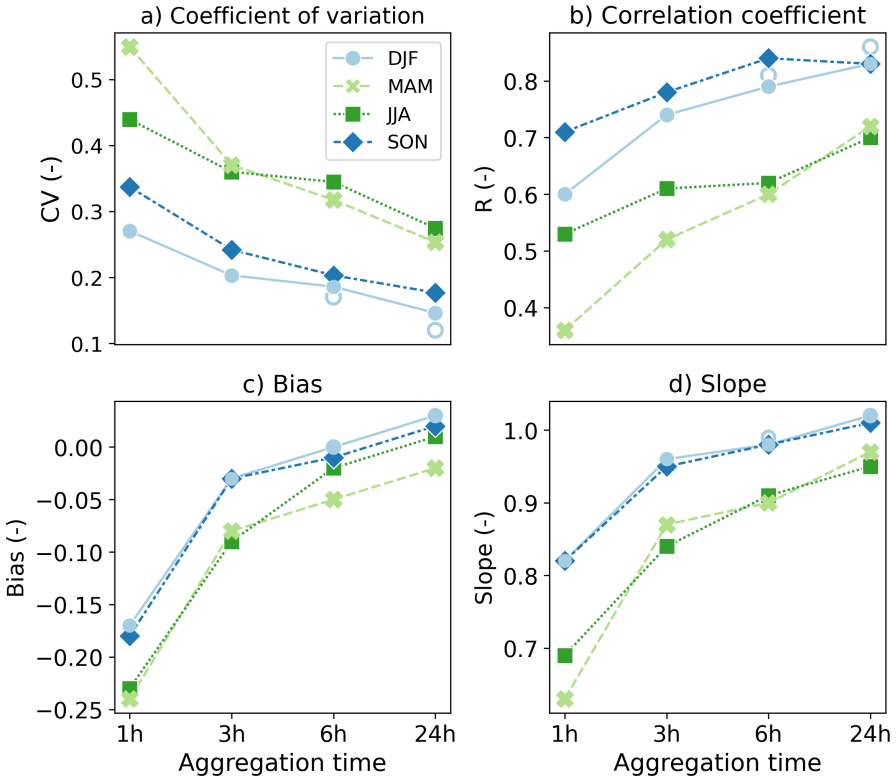

Figure 8. Coefficient of variation (a), correlation coefficient (b), bias (c) and slope (d) of filtered PWS rainfall accumulations against AWS for different seasons and accumulation intervals. Hollow circles indicate the values in winter after applying a temperature filter.

of the rainfall during these events fell within 10 min, exceeding intensities of 75 mm h^{-1} during that interval. However, it is unknown if the rain was evenly spread within these 10 min, or mostly occurred during a shorter period of time and if this measurement range of the PWSs was indeed exceeded.

4.5 Areal reduction effect

Figure 9 shows a substantial decline in ARF with larger area sizes and shorter durations, with largest reductions for short durations. The decline becomes more prominent for longer return periods. For an area of 64 km^2 (based on the average distance of a PWS cluster to the corresponding AWS) and a duration of 1 h, the ARF according to Beersma et al. (2019) varies between 0.89 and 0.83 for return periods of 2 and 50 years, respectively, while for 24 h the ARF varies between 0.96 and 0.93 for return periods of 2 and 50 years, respectively. The larger areal reductions for shorter intervals are also visible in the average bias in Fig. 9.

https://doi.org/10.5194/egusphere-2024-3207
Preprint. Discussion started: 8 November 2024

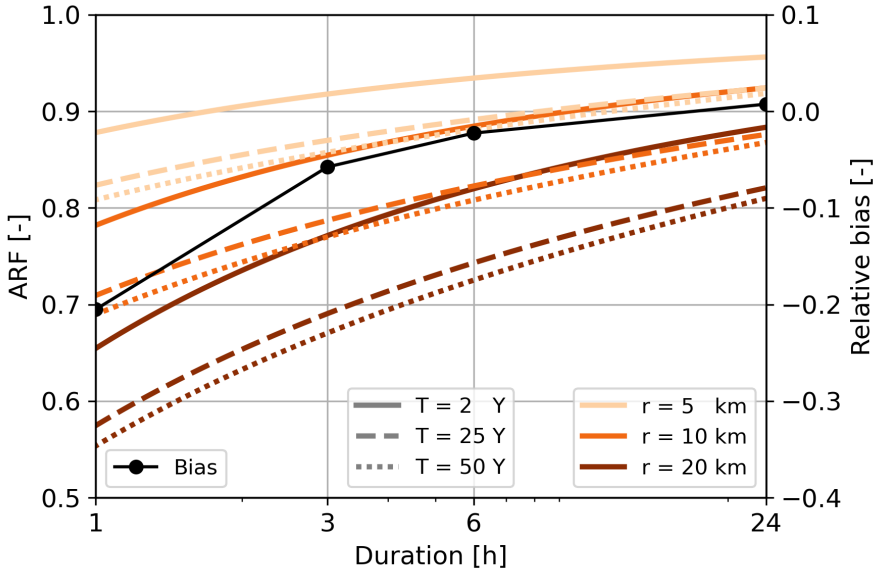

Figure 9. Areal reduction factor (left y-axis) as function of duration for area sizes with a radius of 5, 10 and 20 km (converted to an area) and return periods of T = 2, 25 and 50 years. The right y-axis shows the averaged relative bias per duration.

5 Discussion

5.1 Bias correction factor

A significant bias is present in the PWS dataset. From De Vos (2019) a bias correction factor of 1.13 came out for a 1-month dataset covering the Netherlands, which is different from the 1-year calibration set from the same study for Amsterdam only (MFBC of 1.24), which is part of the PWSQC algorithm and was used in this study. Alternatively, Overeem et al. (2024a) used a MFBC of 1.063 for a pan-European dataset. Neither of the MFBC factors (1.063 or 1.13) would have been able to fully compensate for the bias present in the dataset used in this research. This difference might be caused by two main reasons. First, both MFBC factors were based on different reference datasets. De Vos et al. (2019) utilized gauge-adjusted radar values. Radars indirectly measure rainfall, which might not be representative for rainfall at the ground. In addition, radars do not measure on a grid, rather the values are interpolated, adding extra uncertainty. Spatially adjusting radars with rain gauges improves the overall quality, however, substantial errors remain. Secondly, this research focused on the highest rainfall events over a longer period of time, while both De Vos et al. (2019) and Overeem et al. (2024a) did not distinguish between certain types of rain events, rather looking at a full month or year of rainfall. The performance of tipping buckets is a non-linear function of rainfall intensity (Niemczynowicz, 1986; Humphrey et al., 1997). It requires time for the tipping bucket mechanism to reposition itself after a tip. Higher intensities enhance this problem, resulting in an increased undercatch. Therefore, the type of dataset and the

https://doi.org/10.5194/egusphere-2024-3207
Preprint. Discussion started: 8 November 2024

included rainfall events play a role in the performance. Applying a MFBC factor of 1.24 over the dataset almost eliminates the bias for accumulation intervals of 24 h. The remaining bias in 1 h intervals may be attributed to predominating high-intensities.

5.2 Quality control

The quality control algorithm from De Vos (2019) utilized in this research improves the overall performance of the PWSs (see supporting information, Fig.B1). However, there are some limitations to this algorithm. The algorithm works only if there are enough neighbouring stations within 10 km, limiting the usefulness for less densely populated regions. That said, for this study only a small percentage (0.66%) was discarded from this dataset due to an insufficient number of neighbouring PWSs. While the number of currently active PWSs is quite high in Europe, they are not evenly distributed (see Fig.1 for the network density of PWSs across Europe). For that reason, regions with a less dense network of PWSs are expected to have a higher percentage of discarded stations due to insufficient neighbours (around 35% within Europe). Alternatively, other data sources (such as gauges or weather radars operated by national meteorological or hydrological services) can be employed for quality control, such as employed in the QC algorithm by Bárdossy et al. (2021). In addition, insufficiently calibrated PWSs which record higher rainfall at each time stamp, are not discarded by the HI filter if a certain threshold is not reached. These differences become more apparent when accumulated over longer periods. With a dynamic bias correction factor this could have been adjusted.

Another limitation of a quality control algorithm that does not use auxiliary data is that if all PWSs provide faulty observations, these timestamps are not flagged, consequently giving a wrong signal. This was observed for two events during winter for 6 and 24 h accumulation intervals, when none of the stations recorded any precipitation during an event, while the AWSs did observe precipitation (e.g. Fig. 7c). During winter, solid precipitation can occur, which can result in an undercatch by the PWSs, as these are not heated and consequently work best for temperatures above freezing point. Results from Overeem et al. (2024a) also suggested that PWSs are not able to capture solid precipitation. Quality control algorithms based on a reference dataset, such as from Bárdossy et al. (2021), would have filtered these PWSs. Alternatively, a temperature filter could be developed, without using auxiliary weather stations. The temperature module present at the PWS can be utilized for this.

5.3 Spatial sampling errors

The decorrelation distance of rainfall is typically much higher in winter compared to summer in the Netherlands. Specifically, for shorter aggregation times this holds (Van de Beek et al., 2012; Van Leth et al., 2021). The average distance of around 4.5 km from a PWS cluster towards the closest AWS was below the decorrelation distance corresponding to a 1-h aggregation interval found by Van Leth et al. (2021) and Van de Beek et al. (2012). While this limits the errors related to spatial sampling, it is expected that this effect remains most pronounced for events in summer and at shorter aggregation intervals (i.e. 1 h). Lowering the radius reduces the number of available PWSs and consequently increases the uncertainty. From the error bars in Fig. 7 variation within a cluster of PWSs was observed, with the largest variation found in spring and summer. For very small-scale convective rainfall events the distance towards the closest AWS might still have been too large, resulting in variations of the observed rainfall by the PWSs nearby. This is also visible from the ARF in Fig. 9, which declines more for rarer events.

https://doi.org/10.5194/egusphere-2024-3207
Preprint. Discussion started: 8 November 2024

5.4 Uncertainty of AWSs

The 10-min AWS dataset is used as a reference, however, it is not an absolute truth. Brandsma (2014) compared the AWS network and manual rain gauge network over the Netherlands and concluded that the AWS network underestimates rainfall with 5-8% annually, with higher underestimation in winter (7.7%) than summer (5.0%). The undercatch is nonlinear with intensity, with larger intensities resulting in less underestimation. These uncertainties are not taken into account in this research.

6 Conclusions

This study provides insight into the uncertainty arising from personal weather stations (PWSs) rainfall estimates during high-intensity rainfall events, by performing a systematic long-term analysis. The analysis focuses on the most intense rainfall observations for a large number of events (1760) over six years (2018-2023) in the Netherlands. PWS data were evaluated against rainfall measurements from automatic weather stations (AWSs). These events were selected over different meteorological seasons (winter, spring, summer, autumn), durations (1, 3, 6 and 24 h) and AWSs (11 locations spread over the country). While PWSs are subject to connection failure which reduces data availability, around 96% of the stations were available over all events. PWS data were filtered with a quality control (QC) algorithm, utilizing neighbouring PWSs. After QC, around 88% of the original dataset was kept. Metrics were calculated over a cluster of PWSs, rather than individual stations, reducing the impact of uncertainties arising from single stations.

Results showed that PWSs severely underestimate rainfall. However, applying a mean field bias correction (MFBC) factor of 1.24 as part of the PWSQC algorithm substantially reduces this bias for intervals of 3 h and longer, indicating that the MFBC of 1.063 by Overeem et al. (2024a) (European dataset) and 1.13 proposed by De Vos et al. (2019) (Netherlands dataset) are not able to account for high-intensity rainfall events. A seasonal effect is visible in the bias, specifically for shorter accumulation intervals, with largest biases for summer and spring. This seasonal and temporal dependence is also seen from the correlation coefficient (r), coefficient of variation (CV) and the slope of the fitted linear regression line. Outliers in winter seemed to have been caused by freezing temperatures (solid precipitation). For that reason, it is recommended to further analyse the impact of temperature or solid precipitation on the performance of the PWS. The temperature module available in PWSs can be used for this. In addition, PWSs were not able to capture the most intense rainfall events, with high intensities over a relative short amount of time (e.g. > 75 mm h^{-1} within 10 min). These highest intensities occurred during summer and spring, with events that typically occur once in 10 years or even longer return periods. Rain gauges from PWSs used in this research utilize a tipping bucket mechanism, which are known to suffer from non-linear underestimation errors with increasing intensities, potentially causing these outliers. In addition, the spatial footprint of these high-intensity rainfall events is unknown, potentially influencing errors related to spatial sampling due to the average distance of 4.5 km towards the nearest AWS. The areal reduction factor shows a strong decline for longer return periods, which partially explains the larger bias for rarer events, such as events with a return period of 50 years, for which the reduction can be up to 17% for 1 h durations. This reduction decreases to 7.0% for a duration of 24 h. Performance of the PWSs improved over longer accumulation intervals, resulting in a r of 0.83 and 0.83 and a CV of 0.15 and 0.18 for 24 h for winter and autumn, respectively.

https://doi.org/10.5194/egusphere-2024-3207
Preprint. Discussion started: 8 November 2024

With the high density of PWSs in the Netherlands (around 1 PWS per 9 km^2), there is a clear potential of using PWSs. This will also be the case for other regions in Europe that have a relative high coverage of PWSs. The accuracy however depends on the desired temporal resolution, season and intensity. Although applying a MFBC factor reduces or even completely compensates for the underestimation, we recommend to further investigate the dynamic response of these stations at different intensities to enable dynamic calibration and consequently minimize non-linear errors related to this.

Code and data availability. The automatic weather stations from the Royal Netherlands Meteorological Institute (KNMI) is freely available on the KNMI data platform for 10 min intervals: https://dataplatform.knmi.nl/dataset/neerslaggegevens-1-0. The hourly validated dataset is available at: https://www.daggegevens.knmi.nl/klimatologie/uurgegevens. Part of the quality control of the Netatmo gauge data, i.e. the faulty zeroes and high-influx filters, are based on the PWSQC algorithm written in R language and can be found at: https://github.com/LottedeVos/PWSQC. Dataset with Netatmo PWS rainfall data can be found at: https://doi.org/10.4121/caa0a93a-effd-4574-95ec-cd874ca97c05.v1 (Rombeek et al., 2024).

https://doi.org/10.5194/egusphere-2024-3207
Preprint. Discussion started: 8 November 2024

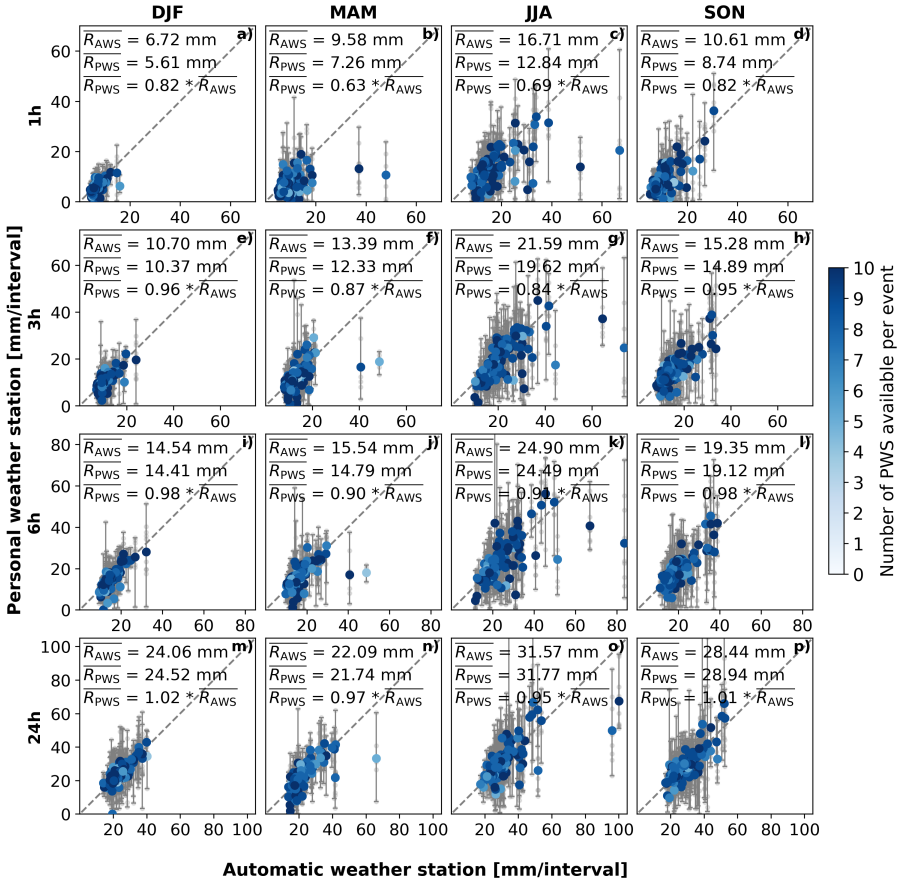

Figure A1. Scatter plots of filtered PWS rainfall accumulations against AWS for the winter (a, e, i and m), spring (b, f, j and n), summer (c, g, k and o) and autumn (d, h, l and p) seasons and accumulation intervals of 1 h (a-d), 3 h (e-h), 6 h (i-l) and 24 h (m-p). The large blue dots indicate the average of a cluster of PWS against one AWS, the vertical bars indicate the minimum and maximum of that cluster of PWSs. The blue gradient indicates the number of PWSs used to calculate the mean, minimum and maximum rainfall. The small grey dots resemble one individual PWS against an AWS. The $\overline{R_{\mathrm{AWS}}}$ and $\overline{R_{\mathrm{PWS}}}$ represent the average rainfall over the selected events recorded by the AWS and PWS, respectively. $\overline{R_{\mathrm{PWS}}} = a * \overline{R_{\mathrm{AWS}}}$ represents the linear regression line, fitted through zero, with a indicating the slope.

https://doi.org/10.5194/egusphere-2024-3207
Preprint. Discussion started: 8 November 2024

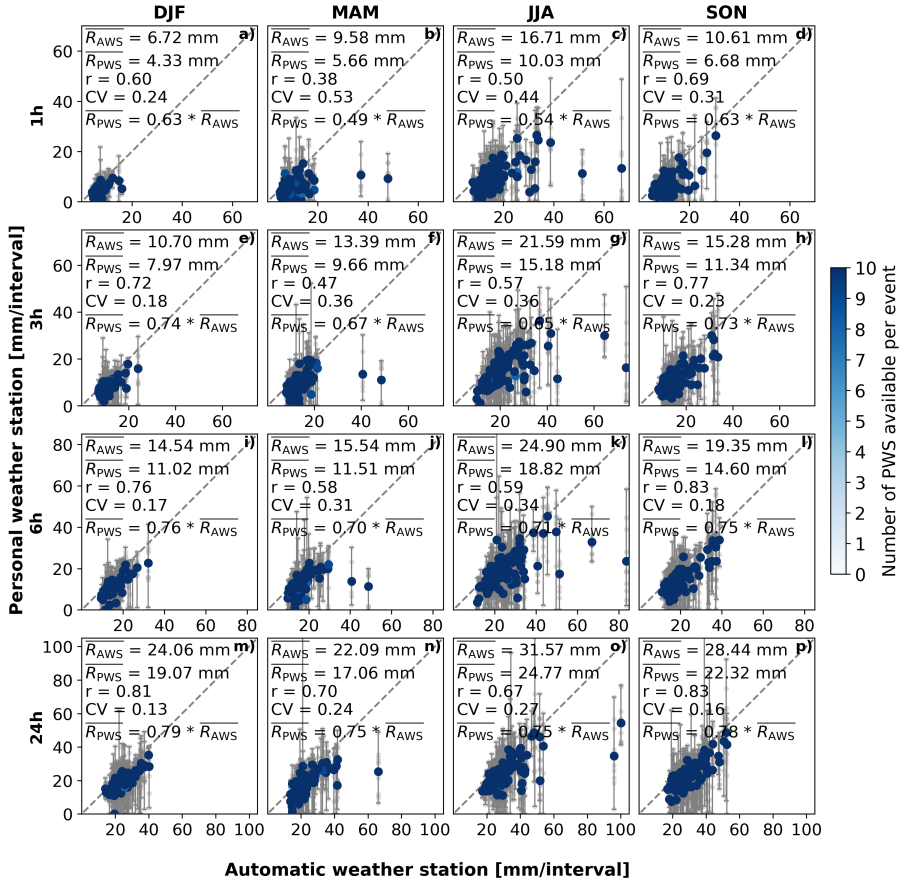

Figure B1. Scatter plots of raw PWS rainfall accumulation data against AWSs for the winter (a, e, i and m), spring (b, f, j and n), summer (c, g, k and o) and autumn (d, h, l and p) seasons and accumulation intervals of 1 h (a-d), 3 h (e-h), 6 h (i-l) and 24 h (m-p). The large blue dots indicate the average of a cluster of PWS against one AWS, the vertical bars indicate the minimum and maximum of that cluster of PWSs. The blue gradient indicates the number of PWSs used to calculate the mean, minimum and maximum rainfall. The small grey dots resemble one individual PWS against an AWS. The $\overline{R_{\mathrm{AWS}}}$ and $\overline{R_{\mathrm{PWS}}}$ represent the average rainfall over the selected events recorded by the AWS and PWS, respectively. *r* and CV indicate the correlation coefficient and the coefficient of variation. $\overline{R_{\mathrm{PWS}}} = a * \overline{R_{\mathrm{AWS}}}$ represents the linear regression line, fitted through zero, with a indicating the slope.

Appendix A: Overview of all seasons and accumulation intervals

Appendix B: Raw PWS data

Author contributions. NR: conceptualization, data curation, formal analysis, investigation, methodology, software, validation, visualisation, writing. MH: conceptualization, funding acquisition, methodology, writing (review & editing). AD: software, writing (review & editing). RU: conceptualization, funding acquisition, methodology, writing (review & editing)

https://doi.org/10.5194/egusphere-2024-3207
Preprint. Discussion started: 8 November 2024

Competing interests. One of the authors (MH) is member of the editorial board of HESS.

Acknowledgements. The authors would like to thank Davide Wüthrich for discussions and for proofreading the manuscript and Claudia Brauer for providing insightful feedback on the results, which helped to improve this paper. This work is part of the Perspectief research programme Future flood risk management technologies for rivers and coasts with project number P21-23. This programme is financed by Domain Applied and Engineering Sciences of the Dutch Research Council (NWO).

https://doi.org/10.5194/egusphere-2024-3207
Preprint. Discussion started: 8 November 2024

References

Arnaud, P., Lavabre, J., Fouchier, C., Diss, S., and Javelle, P.: Sensitivity of hydrological models to uncertainty in rainfall input, Hydrological Sciences Journal–Journal des Sciences Hydrologiques, 56, 397–410, 2011.

Bárdossy, A., Seidel, J., and El Hachem, A.: The use of personal weather station observations to improve precipitation estimation and interpolation, Hydrology and Earth System Sciences, 25, 583–601, https://doi.org/10.5194/hess-25-583-2021, 2021.

Beersma, J., Hakvoort, H., Jilderda, R., Overeem, A., and Versteeg, R.: Neerslagstatistiek en-reeksen voor het waterbeheer 2019, vol. 19, STOWA, 2019.

Berne, A., Delrieu, G., Creutin, J.-D., and Obled, C.: Temporal and spatial resolution of rainfall measurements required for urban hydrology, Journal of Hydrology, 299, 166–179, 2004.

Beven, K.: Facets of uncertainty: epistemic uncertainty, non-stationarity, likelihood, hypothesis testing, and communication, Hydrological Sciences Journal, 61, 1652–1665, 2016.

Brandsma, T.: Comparison of automatic and manual precipitation networks in the Netherlands, KNMI, 2014.

Brandsma, T., Beersma, J., van den Brink, J., Buishand, T., Jilderda, R., and Overeem, A.: Correction of rainfall series in the Netherlands resulting from leaky rain gauges, Tech. rep., Technical Report TR-387. De Bilt: KNMI, 2020.

Brousse, O., Simpson, C. H., Poorthuis, A., and Heaviside, C.: Unequal distributions of crowdsourced weather data in England and Wales, Nature Communications, 15, 1–11, 2024.

Colli, M., Lanza, L., La Barbera, P., and Chan, P.: Measurement accuracy of weighing and tipping-bucket rainfall intensity gauges under dynamic laboratory testing, Atmospheric research, 144, 186–194, 2014.

Cristiano, E., ten Veldhuis, M.-C., and Van De Giesen, N.: Spatial and temporal variability of rainfall and their effects on hydrological response in urban areas–a review, Hydrology and Earth System Sciences, 21, 3859–3878, 2017.

De Vos, L., Leijnse, H., Overeem, A., and Uijlenhoet, R.: The potential of urban rainfall monitoring with crowdsourced automatic weather stations in Amsterdam, Hydrology and Earth System Sciences, 21, 765–777, 2017.

De Vos, L. L.: Rainfall observations datasets from Personal Weather Stations, 4TU.ResearchData, https://doi.org/10.4121/uuid:6e6a9788-49fc-4635-a43d-a2fa164d37ec, 2019.

De Vos, L. W., Leijnse, H., Overeem, A., and Uijlenhoet, R.: Quality control for crowdsourced personal weather stations to enable operational rainfall monitoring, Geophysical Research Letters, 46, 8820–8829, 2019.

De Vries, H. and Selten, F.: Zomer Bijna Net Zo Nat Als Winter, https://www.knmi.nl/over-het-knmi/nieuws/zomer-bijna-net-zo-nat-als-winter, published: 25 May 2023, 2023.

El Hachem, A., Seidel, J., O'Hara, T., Villalobos Herrera, R., Overeem, A., Uijlenhoet, R., Bárdossy, A., and de Vos, L.: Overview and comparison of three quality control algorithms for rainfall data from personal weather stations, Hydrology and Earth System Sciences, 2024, in press.

European Environment Agency: Impervious Built-up 2018 (raster 10 m), Europe, 3-yearly, Aug. 2020, https://doi.org/10.2909/3e412def-a4e6-4413-98bb-42b571afd15e, 2020.

Habib, E., Krajewski, W. F., and Kruger, A.: Sampling errors of tipping-bucket rain gauge measurements, Journal of Hydrologic Engineering, 6, 159–166, 2001.

Hrachowitz, M. and Weiler, M.: Uncertainty of precipitation estimates caused by sparse gauging networks in a small, mountainous watershed, Journal of Hydrologic Engineering, 16, 460–471, 2011.

https://doi.org/10.5194/egusphere-2024-3207
Preprint. Discussion started: 8 November 2024

Humphrey, M., Istok, J., Lee, J., Hevesi, J., and Flint, A.: A new method for automated dynamic calibration of tipping-bucket rain gauges, Journal of Atmospheric and Oceanic Technology, 14, 1513–1519, 1997.

Imhoff, R., Brauer, C., Overeem, A., Weerts, A., and Uijlenhoet, R.: Spatial and temporal evaluation of radar rainfall nowcasting techniques on 1,533 events, Water Resources Research, 56, e2019WR026 723, 2020.

KNMI: Climate Viewer, https://www.knmi.nl/klimaat-viewer/grafieken-tabellen/meteorologische-stations/stations-maand/stations-maand_1991-2020, last accessed: 3 July 2024, 2024.

Krajewski, W. F., Villarini, G., and Smith, J. A.: Radar-rainfall uncertainties: Where are we after thirty years of effort?, Bulletin of the American Meteorological Society, 91, 87–94, 2010.

Lobligeois, F., Andréassian, V., Perrin, C., Tabary, P., and Loumagne, C.: When does higher spatial resolution rainfall information improve streamflow simulation? An evaluation using 3620 flood events, Hydrology and Earth System Sciences, 18, 575–594, https://doi.org/10.5194/hess-18-575-2014, 2014.

Marsalek, J.: Calibration of the tipping-bucket raingage, Journal of Hydrology, 53, 343–354, 1981.

McMillan, H. K., Westerberg, I. K., and Krueger, T.: Hydrological data uncertainty and its implications, Wiley Interdisciplinary Reviews: Water, 5, e1319, 2018.

Moulin, L., Gaume, E., and Obled, C.: Uncertainties on mean areal precipitation: assessment and impact on streamflow simulations, Hydrology and Earth System Sciences, 13, 99–114, 2009.

Netatmo: Smart Rain Gauge, https://www.netatmo.com/en-eu/smart-rain-gauge, last accessed: June 2024, 2024a.

Netatmo: Welcome aboard, https://dev.netatmo.com/apidocumentation, last accessed: June 2024, 2024b.

Nielsen, J., van de Beek, C., Thorndahl, S., Olsson, J., Andersen, C., Andersson, J., Rasmussen, M., and Nielsen, J.: Merging weather radar data and opportunistic rainfall sensor data to enhance rainfall estimates, Atmospheric Research, 300, 107 228, 2024.

Niemczynowicz, J.: The dynamic calibration of tipping-bucket raingauges, Hydrology Research, 17, 203–214, 1986.

Niemczynowicz, J.: Urban hydrology and water management–present and future challenges, Urban water, 1, 1–14, 1999.

Ochoa-Rodriguez, S., Wang, L.-P., Gires, A., Pina, R. D., Reinoso-Rondinel, R., Bruni, G., Ichiba, A., Gaitan, S., Cristiano, E., van Assel, J., et al.: Impact of spatial and temporal resolution of rainfall inputs on urban hydrodynamic modelling outputs: A multi-catchment investigation, Journal of Hydrology, 531, 389–407, 2015.

Overeem, A., Buishand, T., and Holleman, I.: Extreme rainfall analysis and estimation of depth-duration-frequency curves using weather radar, Water Resources Research, 45, 2009.

Overeem, A., Buishand, T., Holleman, I., and Uijlenhoet, R.: Extreme value modeling of areal rainfall from weather radar, Water Resources Research, 46, 2010.

Overeem, A., Leijnse, H., van der Schrier, G., van den Besselaar, E., Garcia-Marti, I., and De Vos, L. W.: Merging with crowdsourced rain gauge data improves pan-European radar precipitation estimates, Hydrology and Earth System Sciences, 28, 649–668, https://doi.org/10.5194/hess-28-649-2024, 2024a.

Overeem, A., Uijlenhoet, R., and Leijnse, H.: Quantitative precipitation estimation from weather radars, personal weather stations and commercial microwave links, in: Advances in Weather Radar. Volume 3, edited by Bringi, V., Mishra, K., and Thurai, M., vol. 3, pp. 27–68, Institution of Engineering and Technology, https://doi.org/10.1049/SBRA557H_ch2, 2024b.

Rombeek, N., Hrachowitz, M., Droste, A. M., and Uijlenhoet, R.: Rainfall observations dataset from personal weather stations around automatic weather stations in the Netherlands, https://doi.org/10.4121/caa0a93a-effd-4574-95ec-cd874ca97c05.v1, 2024.

https://doi.org/10.5194/egusphere-2024-3207
Preprint. Discussion started: 8 November 2024

Shedekar, V. S., Brown, L. C., Heckel, M., King, K. W., Fausey, N. R., and Harmel, R. D.: Measurement errors in tipping bucket rain gauges under different rainfall intensities and their implication to hydrologic models, in: 2009 Reno, Nevada, June 21-June 24, 2009, p. 1, American Society of Agricultural and Biological Engineers, 2009.

Thorndahl, S., Einfalt, T., Willems, P., Nielsen, J. E., Ten Veldhuis, M.-C., Arnbjerg-Nielsen, K., Rasmussen, M. R., and Molnar, P.: Weather radar rainfall data in urban hydrology, Hydrology and Earth System Sciences, 21, 1359–1380, 2017.

Uijlenhoet, R. and Berne, A.: Stochastic simulation experiment to assess radar rainfall retrieval uncertainties associated with attenuation and its correction, Hydrology and Earth System Sciences, 12, 587–601, 2008.

Van de Beek, C., Leijnse, H., Torfs, P., and Uijlenhoet, R.: Seasonal semi-variance of Dutch rainfall at hourly to daily scales, Advances in Water Resources, 45, 76–85, 2012.

Van Leth, T. C., Leijnse, H., Overeem, A., and Uijlenhoet, R.: Rainfall Spatiotemporal Correlation and Intermittency Structure from Micro-γ to Meso-β Scale in the Netherlands, Journal of Hydrometeorology, 22, 2227–2240, 2021.

Villarini, G. and Krajewski, W. F.: Review of the different sources of uncertainty in single polarization radar-based estimates of rainfall, Surveys in Geophysics, 31, 107–129, 2010.

Villarini, G., Mandapaka, P. V., Krajewski, W. F., and Moore, R. J.: Rainfall and sampling uncertainties: A rain gauge perspective, Journal of Geophysical Research: Atmospheres, 113, 2008.